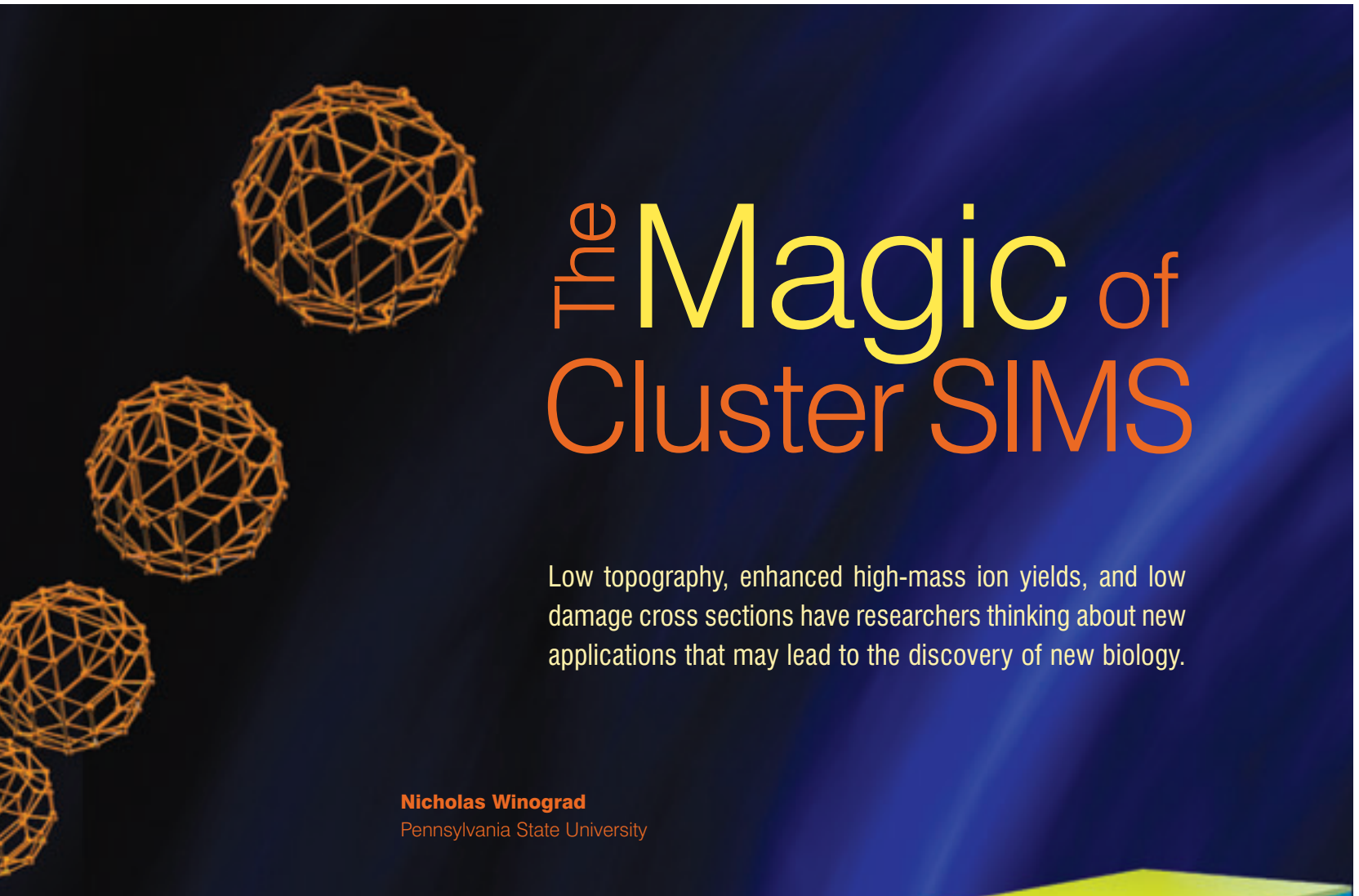

# The Magic of Cluster SIMS

Low topography, enhanced high-mass ion yields, and low damage cross sections have researchers thinking about new applications that may lead to the discovery of new biology.

**Nicholas Winograd**
Pennsylvania State University

Every once in a while, a breakthrough propels a mature field into new dimensions—just as the discoveries of MALDI and ESI opened MS to biologists and, incidentally, racked up Nobel Prizes for their inventors. This sort of metamorphosis is currently under way in bioimaging because of the remarkable properties of cluster ion beam sources being used with secondary ion MS (SIMS).

These sources direct a beam of energetic ions (typically several thousand electron volts) at the target; the ions initiate a cascade of moving particles, causing desorption of secondary molecular ions. The two most significant features of this approach are that desorbed molecules arise specifically from the top portion of the sample, making it useful for surface analysis, and that the primary ion beam can be focused to a submicrometer-sized spot where, in conjunction with TOF detection, images of the surface can be obtained.

Because mass spectral information is associated with each pixel, molecule-specific pictures can be acquired. This article will review the "magical" properties of cluster ion sources for SIMS experiments and consider the scope of new applications, particularly in bioimaging.

## TOF-SIMS and the expanding world of MS

The desorption of molecules induced by ion bombardment was first observed >30 years ago. This technique was one of the earliest schemes for detecting organic molecules that were not amenable to electron impact ionization, which, at that time, was the only option for this type of analysis (*1*). The approach has some fundamental flaws, however, and has been eclipsed by MALDI and ESI in recent years. The major weakness is that the bombardment process causes a lot of damage to the sample surface. If the dose is too high (>~1% of the number of surface molecules), a carbon residue from molecular fragmentation builds up on the surface and the signal disappears. This 1% restriction, the so-called static limit, obviously puts a damper on detecting very small sample concentrations.

This problem was addressed during the 1980s by using fast atom bombardment and by dissolving the sample in a liquid matrix so that the surface could be continually regenerated (*2*). The very nature of the desorption process, however, still leads to complicated spectra, congested by matrix and fragment ions created during the impact of the primary particle with the target. Moreover, the mass range is limited to fairly small molecules with a molecular weight less than several thousand daltons. With MALDI or ESI, not only do the spectra consist primarily of molecular ions without fragments, but it is feasible to detect ions with a mass range extending to millions of daltons, thereby opening up the assay to peptides, proteins, and DNA (*3*, *4*). Imaging with MALDI has also been demonstrated, although the effective lateral resolution is, so far, limited to tens of micrometers.

With these difficulties, why is SIMS still being pursued as a viable option for MS measurements? The answer is surface sensitivity and submicrometer imaging capability. In addition, no matrix is required—samples can be studied in "as-received" condition. SIMS is one of the best ways to characterize organic thin films, polymer surfaces, semiconductor surfaces, and a host of other related materials (*5*). In many cases, the lateral resolution is in the 100-nm range. With SIMS, it may be possible to examine patterned surfaces, various arrays, and even single biological cells, all with the molecular specificity unique to MS. Hence, researchers have been willing to put up with mass spectra of less than stellar quality as a trade-off for access to a unique class of samples.

Many of these restrictions are changing with the introduction of primary ion beam sources composed of molecular clusters rather than single atomic particles. These sources greatly simplify SIMS spectra and exhibit an extended mass range for desorbed molecules. Accumulated damage appears to be much less of an issue, and in some cases it is possible to exceed the static limit, thereby increasing sensitivity. Cluster sources with imaging capability are just now entering the marketplace. There is a sense that the field is indeed poised for one of those unusual jumps in performance that can open new vistas.

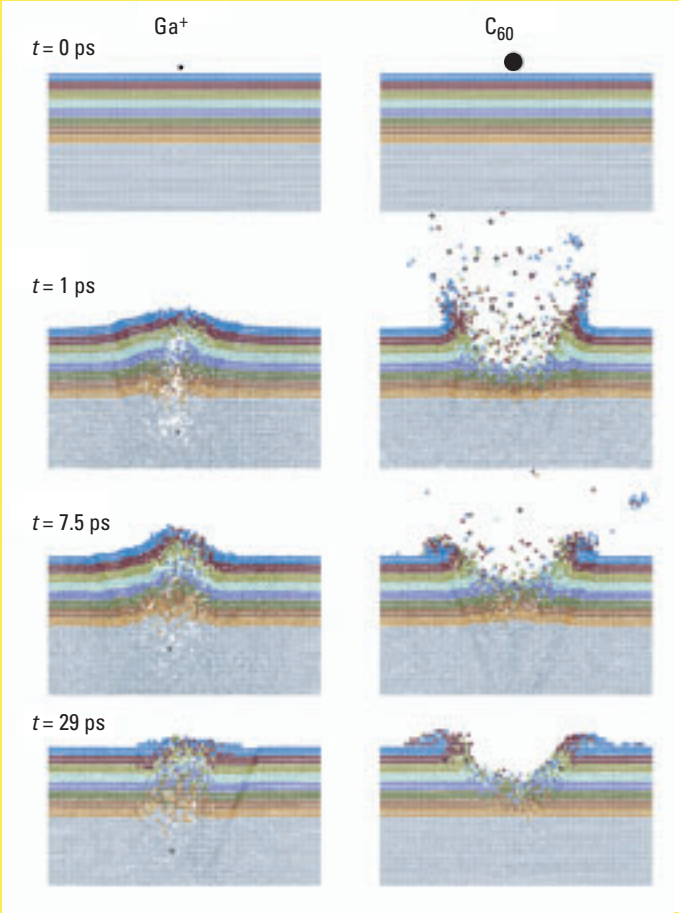


**FIGURE 1.** Impacted silver.

Snapshots from a molecular dynamics computer simulation of 15-keV $C_{60}$ and 15-keV $Ga^+$ bombardment of silver metal. The view is from the side of a portion of a 10 × 10 × 10 $nm^3$ microcrystallite containing 612,000 atoms. Sputtered silver atoms induced by $Ga^+$ bombardment are not visible because they are ejected at an angle out of the slab. The layers are colored so that atomic displacements are more easily visible. (Adapted from Ref. 6.)

## Cluster ion sources work their magic

Before the special effects associated with cluster bombardment are described, it is useful to have a picture of how desorption occurs during atomic bombardment. These pictures are created from molecular dynamics computer simulations of the ion-bombardment event (*6*). These types of calculations have been developed over many years and are available primarily for metallic targets, although a lot of recent effort has been devoted to the behavior of organic thin films. A typical trajectory of a 15-keV $Ga^+$ bombardment of a silver crystal surface is shown

in Figure 1. The time sequence shows that a considerable disruption occurs deep into the crystal and around the impact point. Very little material is removed from the solid, in part because the energy is deposited so far below the surface.

Clusters of atoms behave very differently. For example, consider bombarding the silver surface with a 15-keV $C_{60}$ buckminsterfullerene, instead of $Ga^+$. In this case, each carbon atom in this cluster would have a kinetic energy (KE) of 15,000/60 or 250 eV. This energy is much greater than the C–C bond strength in $C_{60}$ of ~5 eV, so one might expect that the buckyball would be completely shattered upon impact. As a consequence, the solid might react as though 60 individual 250-eV carbon atoms hit it simultaneously, each creating its own cascade of moving atoms. The fact that the KE of 250 eV per atom in the cascade is much lower than the 15,000 eV associated with $Ga^+$ suggests that the deposited energy will remain closer to the surface, more effectively leading to desorption.

A computer simulation of a $C_{60}$ impact on silver is shown in Figure 1. These are rather heroic calculations because they require modeling >600,000 silver atoms to contain the trajectory within the model microcrystallite. Notice the formation of a crater with mesoscopic dimensions. Nearly 400 atoms are sputtered per incident buckyball, a >15-fold increase over $Ga^+$ bombardment. Although the yield is much higher, the depth of damage is smaller than for the corresponding atomic bombardment, extending only a few layers below the bottom of the crater. These simulations show that a nonlinear enhancement of the yield of silver occurs, which means that the yield from the 15-keV $C_{60}$ bombardment is >60× the yield from 250-eV carbon bombardment. Finally, note that the time of the trajectory is considerably longer for cluster bombardment—29 ps for $C_{60}$ versus 3 ps for gallium. These pictures clearly suggest that when clusters are used, the energy deposition process is quite different than when atomic beams are used.

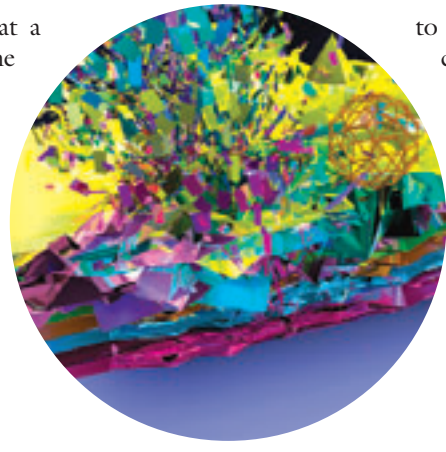

Characterizing **complex multilayer** structures is of **increasing importance,** particularly **to the electronics** industry.

## $Au_3$ and $C_{60}$ projectiles

The fact that cluster ion sources are more effective at desorbing molecules was discovered more than 15 years ago (*7*, *8*). The projectiles $SF_6$ and $Cs_xI_y$ enabled the acquisition of SIMS spectra with enhanced sensitivity for many polymer and organic thin films. The $SF_6$ source was quickly improved and commercialized. Other species, such as aromatic hydrocarbons, massive glycerol clusters, and various inorganic complex ions, were also found to be effective. Although the SIMS community conceded that these sources could significantly improve the quality of data, only a few laboratories aggressively pursued applications. Perhaps the reason for this lapse is that the sources themselves are not conducive to everyday use. Maintenance issues, low beam current, and/or lack of focusing have relegated most of these guns to the back of the drawer.

The emergence of $Au_3$ and $C_{60}$ ion sources has resolved many of these issues and has stimulated a major new push to map all the benefits of cluster ions. The $Au_3$ source utilizes a liquid-metal ion gun (LMIG; *9*, *10*). For traditional SIMS experiments, the LMIG consists of a field emitter tip normally coated with gallium (the choice of projectile for Figure 1). Gallium ions are extracted from the tip and refocused into the sample with a spot size of <50 nm. The ion KE needs to be fairly high to achieve this spot size. Typically, values of 15–40 keV are required.

It is possible to use gold as the coating metal. Early designs had short lifetimes due to the high temperature required to force the gold to coat the emitter tip. It was soon discovered that AuGe or AuSi eutectic alloys could be used at much lower temperatures. Because there is more than one component, the source emits a variety of ions, which necessitates using a mass filter. Even with these issues, a significant intensity of $Au_3$ can still be used for SIMS experiments. The source exhibits a very high brightness, has a lifetime >500 h, and can be focused to a spot size of ~200 nm. This source has become very popular, and most instruments have already been retrofitted to accept it.

The $C_{60}$ source has a more conventional design. A stable vapor pressure for $C_{60}$ can be created by heating the source to ~300 °C. The vapor can then be very efficiently ionized by conventional electron impact (*11*). When high-quality focusing optics have been used, spot sizes of ~2 μm have been obtained, and designs are being discussed for 200-nm operation. This source is robust, exhibits a lifetime of >500 h before cleaning, and has plenty of beam current for SIMS experiments.

These two species appear to have complementary properties. Both ions enhance high-mass ion yields by factors of 100,000 or more. The damage accumulation rate appears to be higher with $Au_3$ than with $C_{60}$ (*11*), which might be expected because the KE of each gold atom is greater than the KE of each carbon atom. Currently, the focusing properties of the gold source are better than those of the $C_{60}$ source, so imaging experiments are more practical with the LMIG design. In any case, both of these projectiles are yielding new applications in a variety of fields.

## Implications for depth profiling

Characterizing complex multilayer structures is of increasing importance, particularly to the electronics industry. When ion beams are used, it is possible to systematically remove material from the sample in a layer-by-layer fashion and subsequently determine the composition of each layer by MS. For atomic ion

sources, variation in yield due to crystallographic effects and beam-induced mixing of the layers limits the best achievable depth resolution. This effect can be minimized in various ways, such as using low ion energy and sample rotation. Although these strategies are successful, they add to the complexity of the measurements.

The computer simulation graphics shown in Figure 1 suggest that the use of projectiles such as $C_{60}$ might allow better depth resolution without the need to resort to such trickery. For example, the fact that very little subsurface damage occurs relative to the atomic bombardment shows that the layers are peeled away in a more uniform fashion. Moreover, because the size of the buckyball is greater than the lattice constant of a typical metal substrate, crystallographic effects where sputtering yields depend upon the nature of the surface structure might not be so serious.

Recent experiments that compared the use of $C_{60}$ and $Ga^+$ sources in the analysis of NiCr multilayers bear out this hypothesis (*12*). A direct bombardment with 15-keV $C_{60}$ produced a crater bottom with a root-mean-square roughness of 2.5 nm versus 100 nm for atomic bombardment. The resulting depth resolution was as good as the best value reported using sample rotation and low-energy bombardment. This consequence is particularly important because higher-energy beams are required if depth-profiling measurements are combined with imaging experiments. So, Magical Property #1 is that the topographical roughening that is normally encountered during erosion experiments seems to be absent when a large cluster such as $C_{60}$ is used.

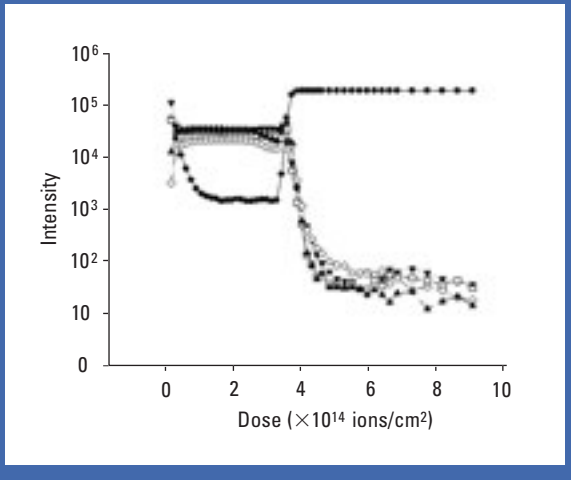


**FIGURE 2.** Secondary ion intensities (log scale) as a function of increasing $SF_5^+$ primary ion dose for PLA films doped with 5% theophylline.

▼, *m/z* 128, PLA fragment $(2n - O)^+$; □, *m/z* 145, PLA fragment $(2n + H)^+$; ◇, *m/z* 165, theophylline $(M + H - O)^+$; ▲, *m/z* 181, theophylline $(M + H)^+$; •, *m/z* 28, $Si^+$; n is the repeat unit of PLA17. (Adapted from Ref. 17.)

## Enhancement of molecular ion yields

Although the advantages of cluster ion sources for observing higher-molecular-weight molecules have been touted for some time, the true significance of the effect has only recently been brought into clear focus by Vickerman and colleagues (*13*, *14*). They showed that the secondary ion yields of molecular ions in the 1000–3000-Da range induced by cluster bombardment are enhanced by at least 300-fold over corresponding atomic bombardment experiments. For several samples, including the small peptide gramicidin D, the molecular ion could only be observed when the cluster source was used. This type of result has been obtained for many classes of organic and inorganic samples. Much-improved SIMS spectra are seen from polymer surfaces such as polystyrene and polyethylene terephthalate. The yields and desorption efficiencies of $C_{60}$ and $Au_3$ have been compared in detail. In general, the ion yield enhancements are about the same for both projectiles, but the desorption efficiency (yield divided by the damage cross section) is significantly higher for $C_{60}$.

The reasons behind this enhancement effect are not yet clear. The computer simulations clearly show that the yield of neutral atoms is higher, and that a propensity exists for bigger sputtered clusters to form. Until calculations are available for molecular solids, however, these types of pictures will not be available for things such as peptides. A few experiments have been performed to compare the amount of material removed with an atomic source and a cluster source. In one case, Langmuir–Blodgett techniques were used to prepare a multilayer structure of known thickness, and the number of incident particles required to remove all the layers was measured (*15*). For molecular weights <~500 Da, the enhancement effect can be largely explained by an increase in the yield of neutral molecules, presumably because of the unusual nature of the collision cascade (Figure 1).

For larger molecules, such experiments have not been possible, and it seems unlikely that the enormous dramatic effects seen by the Vickerman group can be explained solely on the basis of enhanced sputtering. Perhaps the nature of the plume that is formed as the molecules take off is ideally suited to ionization. Perhaps other, unknown mechanisms are at work. This will clearly be an interesting project for future research. So, Magical Property #2 of cluster ion beams, particularly $C_{60}$, is that the usable mass range for SIMS experiments is considerably extended and that the sensitivity for high-mass ions is greatly improved. However, except for a few pathological cases, molecules heavier than 10,000 Da cannot be desorbed intact. The mass range of MALDI and ESI-MS is still much larger than that of cluster SIMS.

## Molecular depth profiling

Another surprise is in store. Typically, the sensitivity of SIMS measurements is limited by the eventual accumulation of damage on the surface of a bombarded solid. This damage is caused either by direct fragmentation of surface molecules by the primary

ion or by displaced lattice atoms just below the surface. Frequently, if an organic film is bombarded long enough, a graphitic overlayer eventually coats it, and all the molecular information is lost. Depth profiling in a fashion analogous to that reported for the NiCr stack discussed earlier has simply not been possible with molecular films. However, for cluster ion beams, the amount of damage accumulation is significantly lower than for atomic projectiles (*16*). The secondary ion formation efficiency is increased even more than the secondary ion yield itself.

This point has been dramatically demonstrated by Gillen et al., who recently reported that the SIMS spectra of small drug molecules doped into a polymer matrix consisting of polylactic acid (PLA) remain stable under $SF_5^+$ cluster ion bombardment (*17*). Very little damage accumulated during the experiment. The result of a typical depth profile for a 5% concentration of theophylline doped into PLA is shown in Figure 2. These particular results are important for examining molecular concentration gradients in polymer films used in drug delivery applications. Molecular stability of this sort has also been observed for histamine dissolved into a water–ice matrix (*18*). Unfortunately, not every molecular solid behaves so nicely, but if the experiments can be generalized, they will have major implications for the analysis of complex multilayer structures.

The reasons behind these observations are still under investigation. One thought is that the enhanced yield associated with cluster bombardment is effective at removing any accumulating chemical damage. For PLA, for example, the polymer unzips during bombardment, resulting in an unusually large sputtering yield. Similarly, for a water–ice matrix, ~2500 water molecules are desorbed for each $C_{60}$ impact, presumably enough to sweep away any chemical fragments left on the surface from a previous impact. Although this explanation is certainly reasonable, the hypothesis will need to be proven so that the conditions for molecular depth profiling can be appropriately optimized.

## Implications for chemical imaging

Imaging with TOF-SIMS is usually performed by a pulsed, focused ion beam scanned across the sample. A TOF mass spectrum is recorded at every point in the image. If special software is used, it is possible to construct an image that displays ion intensity versus position for any mass or set of masses. Depending on the type of beam, the lateral resolution ranges from 50 nm to several micrometers. Although this method is potentially a powerful and unique approach to imaging, it has a fundamental flaw. As the pixel size approaches submicrometer dimensions, the number of molecules available for analysis becomes vanishingly small. For example, there are only 40,000 molecules per layer in a 100-nm spot, corresponding to $6 \times 10^{-20}$ mol. Given the restrictions of static SIMS, only a few hundred of these molecules would be amenable to analysis. This issue has prevented the technology from reaching its full potential.

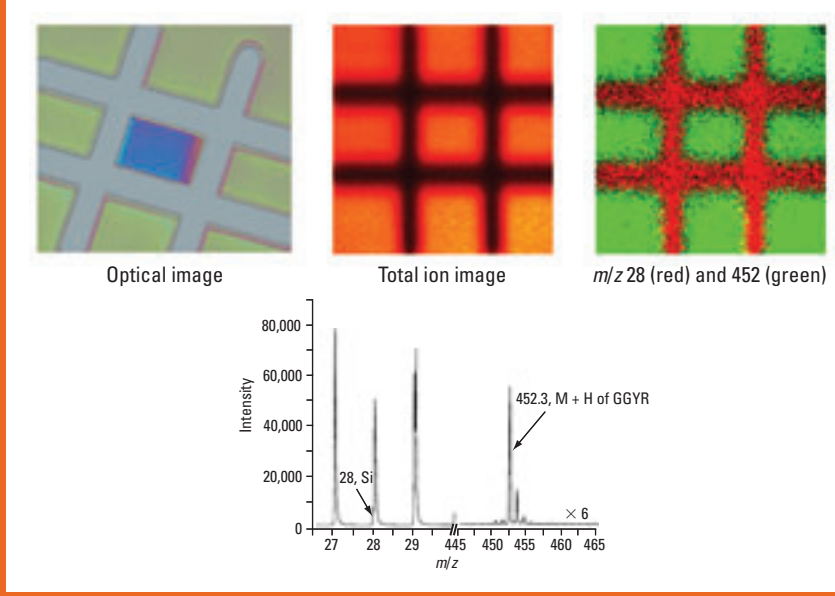


**FIGURE 3.** Tic-tac-toe.

A 300-nm film of Gly–Gly–Tyr–Arg (GGYR) in an array format. The central square has been etched to 150 nm. The change in color in the optical image is caused by the interference effect. The field of view is 520 μm. The spectrum shown corresponds to the total ion image.

At this point, it should be clear where we are heading with cluster SIMS. Because desorption yields and efficiencies are greatly enhanced, there should be a direct benefit to chemical imaging experiments. In Figure 3, a tetrapeptide (Gly–Gly–Tyr–Arg) has been dissolved into the sugar trehalose at the 1% level (*19*). Trehalose is an interesting matrix because peptides retain their folded configuration in a glassy film; the sputtering yield of trehalose under $C_{60}$ bombardment is large enough to allow molecular ion signals to be retained under high-bombardment dose conditions. A 300-nm-thick pad of the peptide on silicon was etched with $C_{60}$ to a 150-nm film thickness. An image of the sample was then acquired where the intensity of the molecular ion at *m/z* 452.3 and the silicon mass at *m/z* 28 were monitored. The resulting image exhibits very high contrast, with as many as 30 counts in each pixel. Such contrast is only possible because the static limit can be

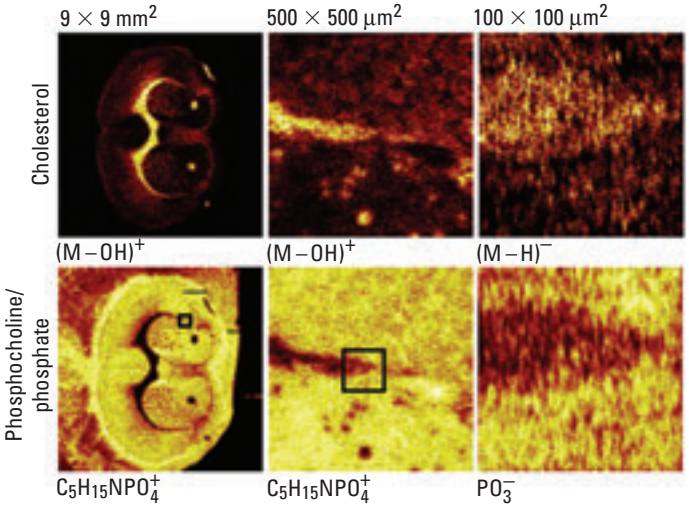


**FIGURE 4.** Mouse brain images.

TOF-SIMS images showing the spatial signal intensity distribution from cholesterol and phosphocholine/phosphate of a section at successively increased magnification. The magnified images were obtained from the areas indicated by the squares in the phosphocholine images. The 9 × 9 $mm^2$ and 500 × 500 $\mu m^2$ images were obtained from measurements of positive secondary ions and show the spatial intensity distribution of the $(M - OH)^+$ peak for cholesterol (369 Da, the most intense positive quasimolecular ion) and the phosphocholine peak ($C_5H_{15}NPO_4^+$); the instrument was optimized for a maximum mass resolution. The 100 × 100 $\mu m^2$ images were obtained from measurements of negative ions and show the intensity distribution of the $(M - H)^-$ peak for cholesterol and the $PO_3^-$ peak; maximum image resolution was 0.2–0.3 µm. (Adapted from Ref. 22.)

exceeded with retention of an intense peptide molecular ion signal. It is technically easy to record these images for various amounts of peptide removed and thus create a 3-D molecular map. So far, only systems that exhibit a very high sputtering yield are amenable to this type of analysis, and each sample needs to be examined on a case-by-case basis. Nonetheless, it is easy to think about many potential applications, including those involving assay of peptide arrays, interlayer mixing in multilayer organic structures, and combinatorial chemistry (*20*).

## Bioimaging of tissue and single cells

Perhaps the most far-reaching application of TOF-SIMS imaging with cluster ion beams is the determination of the lateral distribution of specific substances in biological tissue and cells. MS is a unique approach to this problem, because labeling is not required and the spectra have high molecular specificity. Several studies that use $Au_3^+$ bombardment to determine the lipid distribution in freeze-dried mouse brain have illustrated the power of this approach (*21*, *22*). Molecular ion peaks from cholesterol, sulfatides, phosphatidylinositols, and phosphatidylcholines were all identified in a mass spectral image from several areas of various sizes (Figure 4). Several previous studies have used atomic ion and massive cluster ion bombardment to report on the distribution of the phospholipid headgroup fragment at *m/z* 184 (*16*). However, the mouse brain studies are the first to report that a broad repertoire of ions up to 1000 Da were measured. The availability of these cluster ion sources opens many new possibilities for more of these studies.

Other enormous implications include the ability to examine biological processes on a molecular level and to assess the effects of therapeutic drug treatments on individual cells. Several labs have achieved single-cell bioimaging with atomic primary projectiles (*23–25*). Although the images have been plagued by low signal from the diverse array of membrane molecules, lipid rearrangements at highly curved membrane junctions have been followed. If these types of experiments could be extended to molecules other than phosphatidylcholine fragments and elemental species, much more biochemical information could be acquired. However, SIMS analysis with atomic projectiles is restricted to the section of the cell exposed to the vacuum interface; in other words, examining the vertical molecular distribution of single cells and 3-D imaging is not possible.

The magical properties of cluster SIMS address both of these conundrums. Cluster ion projectiles greatly increase the secondary ion yield, particularly of high-mass fragments and molecular ions. This ability increases not only the mass range of biomolecules amenable to study but also the number of molecules per image pixel. Brighter pixels result in better contrast between adjacent pixels, leading to a more complete and informative chemical map of a single cell. This attribute of $C_{60}$ is nicely depicted by comparing the molecule-specific images taken with an indium atomic primary source and a $C_{60}$ cluster source of a *Spirostomum* cell (Figure 5). *Spirostomum* is a protozoan well known for its ability to contract to one-quarter of its length on a millisecond timescale and for its use in acute toxicity testing. Its large size makes it a particularly attractive cell system for preliminary $C_{60}$ image experiments where the lateral resolution is not as high as that of atomic probes. A quick comparison of the two images establishes that cluster SIMS produces better-quality images than atomic SIMS. The spectra that correspond with these images show that the phosphocholine signal is enhanced ~300-fold with $C_{60}$ versus indium.

In addition to the advantages of enhanced ion yield and improved imaging, $C_{60}$ should be able to depth profile through a cell. Preliminary results from our lab show that the lipid signal remains localized to a freeze-fractured paramecium after $C_{60}$ bombardment. This prospect is tantalizing because cells can be controllably sectioned and molecularly imaged without chemically damaging the molecules of interest or altering their native distribution in the cell. In a Harry Potter-crazed world, everyone needs a little magic, and in the single-cell SIMS community, that magic lies in cluster projectiles.

## Down the road

The properties of cluster SIMS—low topography, enhanced high-mass ion yields, low damage cross sections with molecular

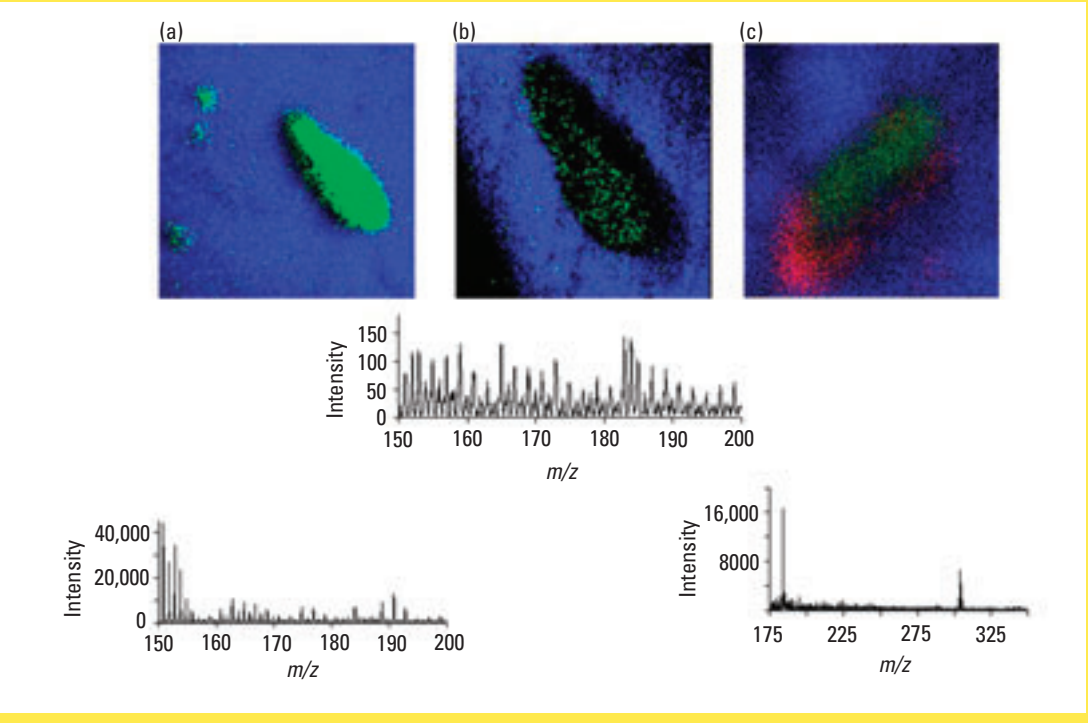


**FIGURE 5.** SIMS images of freeze-dried *Spirostomum* taken with different primary ion sources.

(a) $C_{60}$ probe image and mass spectrum; 700 × 700 μm$^2$ field of view. (b) In-probe image and mass spectrum of (a) in 380 × 380 μm$^2$ field of view. A 300-fold signal increase in *m/z* 184 (phosphocholine) is observed with the $C_{60}$ primary projectile. (c) $C_{60}$ probe image and mass spectrum of freeze-dried *Spirostomum* that was incubated in 0.1 mM cocaine (*m/z* 304); 400 × 400 μm$^2$ field of view. Rapid warming during sample preparation resulted in sublimation of the intracellular material and altered the distribution of cocaine.

depth profiling—are stimulating researchers to think about new applications. As these tools become more commonly available, we anticipate that the unique nature of this methodology will inevitably lead to the discovery of new biology—the specific location of small molecules will be pinpointed with exquisite detail in single cells. Experiments with molecular depth profiling also offer new analysis paradigms for multilayer organic thin films and other complicated structures important to nanotechnology. We are still at an early stage of development in fully realizing the magical properties of cluster SIMS, and not every system behaves as expected. Nonetheless, the guidelines are in place to establish a unique form of 3-D molecular analysis.

Sara Ostrowski and Juan Cheng provided unpublished data for this manuscript and helped invaluably in developing the ideas presented. Funding from the National Science Foundation and the National Institutes of Health is also gratefully acknowledged.

*Nicholas Winograd is a professor at Pennsylvania State University. His research interests focus on ion/solid interactions and bioimaging. Address correspondence about this article to him at 209 Chemistry Bldg., Penn State University, University Park, PA 16802 (nxw@psu.edu).*

## References

(1) Benninghoven, A.; Jaspers, D.; Sichtermann, W. *Appl. Phys.* **1976**, *11*, 35–39.
(2) Barber, M.; et al. *Nature* **1981**, *293*, 270–275.
(3) Karas, M.; Hillenkamp, F. *Anal. Chem.* **1988**, *60*, 2299–2301.
(4) Fenn, J. B.; et al. *Science* **1989**, *246*, 64–71.
(5) Benninghoven, A. *Appl. Surf. Sci.* **2003**, *203*, 1–2.
(6) Postawa, Z.; et al. *J. Phys. Chem. B* **2004**, *108*, 7831–7838.
(7) Blain, M. G.; et al. *Phys. Rev. Lett.* **1989**, *63*, 1625–1628.
(8) Appelhans, A. D.; Delmore, J. E. *Anal. Chem.* **1989**, *61*, 1087–1093.
(9) Davies, N.; et al. *Appl. Surf. Sci.* **2003**, *203*, 223–227.
(10) Kersting, R.; et al. In *Secondary Ion Mass Spectrometry, SIMS XII*, Proceedings of the International Conference on Secondary Ion Mass Spectrometry, Brussels, Belgium, Sept 5–10, 1999; Benninghoven, A., et al., Eds.; Elsevier: Amsterdam, 2000; pp 825–828.
(11) Weibel, D.; et al. *Anal. Chem.* **2003**, *75*, 1754–1764.
(12) Sun, S.; et al. *Appl. Phys. Lett.* **2004**, *84*, 5177–5179.
(13) Wong, S. C. C.; et al. *Appl. Surf. Sci.* **2003**, *203*, 219–222.
(14) Weibel, D. E.; Lockyer, N.; Vickerman, J. C. *Appl. Surf. Sci.* **2004**, *231–232*, 146–152.
(15) Sostarecz, A. G.; et al. *Appl. Surf. Sci.* **2004**, *231–232*, 179–182.
(16) McMahon, J. M.; Dookeran, N. N.; Todd, P. J. *J. Am. Soc. Mass Spectrom.* **1995**, *6*, 1047–1058.
(17) Mahoney, C. M.; Roberson, S., V.; Gillen, G. *Anal. Chem.* **2004**, *76*, 3199–3207.
(18) Wucher, A.; et al. *Appl. Surf. Sci.* **2004**, *231–232*, 68–71.
(19) Cheng, J.; Winograd, N. *Anal. Chem.*, submitted.
(20) Xu, J.; et al. *J. Am. Chem. Soc.* **2004**, *126*, 3902–3909.
(21) Touboul, D.; et al. *Anal. Chem.* **2004**, *76*, 1550–1559.
(22) Sjoevall, P.; Lausmaa, J.; Johansson, B. *Anal. Chem.* **2004**, *76*, 4271–4278.
(23) Colliver, T. L.; et al. *Anal. Chem.* **1997**, *69*, 2225–2231.
(24) Ostrowski, S. G.; et al. *Science* **2004**, *305*, 71–74.
(25) Cliff, B.; et al. *Rapid Commun. Mass Spectrom.* **2003**, *17*, 2163–2167.